International Journal of Engineering Research & Technology (IJERT)
ISSN: 2278-0181
Vol. 3 Issue 2, February - 2014

Pulsed Vortex Flow In Medium – Temperature Range Heat Pipes

A.V. Seryakov

Scientific laboratory, Special Relay System Design and Engineering Bureau,
Nekhinskaya Street, 55, 173021, Velikiy Novgorod, Russia.

The work presents part calculation and part experimental research of the intensification of heat-transfer characteristics of medium-temperature heat pipes. Presented is a vapour jet nozzle, similar to the Laval nozzle, surrounded by a capillary-porous insert along the full length of the heat pipe axial to the direction of heat flow. This increases velocity of the vapour flow, heat-transfer coefficient and pulse rate of two-phase vapour flow.

Medium-temperature range heat pipes, capillary-porous insert, capillary steam injectors, Laval nozzle, condensation sensor.

Heat-transfer efficiency and operational effectiveness of HPs with capillary-porous inserts are defined by closed circulation motion of the working fluid, which undergoes liquid-vapour transition and heat absorption in the evaporation region of the capillary porous insert, vapour phase transfer through a convergent-divergent vapour channel, vapour-liquid transition with heat liberation in the condensation region, and liquid return to the evaporation region through capillary-porous inserts of the HP.

Improvement of the heat-transfer efficiency of heat pipes is a complex task, concerning the device's detailed mechanical design and gas dynamics. Flowing vapour, with microdrops of condensate, appears as a nonlinear flow, with attendant internal processes, such as interphasic heat and mass exchange, and power dissipation [1]. Static regain of supersaturated vapour flow in the condensation region of the heat pipe with turbulator, causes flow stagnation, strong vorticity production near the condensation surface and reverse vapour flow. Thermal load-related processes of vorticity formation and density and pressure fluctuation, proceeding in the vapour channel of heat pipes, are of the utmost interest. For a field research of these processes, stainless steel heat pipes have been manufactured with diethyl ether as the working fluid. The diethyl ether $C_4H_{10}O$ is selected as the main working fluid, which has the boiling temperature under the atmospheric pressure of T_B =35.4°C, freezing temperature T_F = −116.2°C and critical parameters T_C =193.4°C, P_C =3.61MPa. Successful use of diethyl ether as the working fluid for Wilson chambers, on long liquid phase at 140°C, shows its heat resistance, and allows its use as the HP working fluid. Fig.1 shows the HP circuit with flat evaporator, convergent-divergent vapour channel, turbulator and capacitive condensation sensor 8,9. The length of the HP is 100 mm, the diameter is 20 mm [2-3].

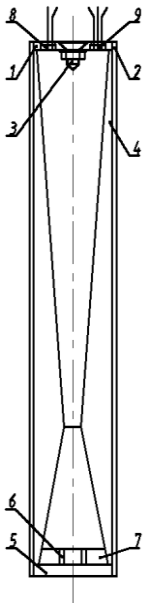

The design presented consists of the metal capillary-porous flat evaporator welded on the flat bottom cover and equipped with injector vapour channels. The channels are oriented at an angle to the longitudinal axis of the pipe and produce swirling vapour flow. In stainless steel HPs with small diameter it is possible to use flat end-plates because of their moderate heat resistance and easy fabrication.

Fig. 1. Heat pipe diagram: 1 – top cover; 2 – cylinder body of the HP; 3 –

cone-shaped turbulator; 4 – capillary-porous insert; 5 – bottom cover; 6 – capillary injector channels, 7 – bottom flat capillary-porous insert-thickness of the condensed layer of the working fluid.

To measure heat flow, HP's condenser regions are arranged in a vortical continuous-flow calorimeter (shown in Fig. 2) with stabilized water flow. For more accurate measurements, the water flow is swirled, the vortex value being fixed. The HP's evaporator is heated using a resistance heater, and the temperature is

Electrical pulses of 10-100 kHz and amplitude 5V are applied to the electrodes of the capacitive sensor 10, Fig.2. The modulation rate is measured via a gain and filtering circuit 12,

evaporator. There are capacitive sensors 8, 9 additionally installed inside the top cover. These sensors measure the

maintained at δT°C higher than the diethyl ether boiling temperature of 35.4°C. The heater temperature is stabilized, and the overheat value of the evaporator is determined within the range of δT = 0-15K. However, the heating power of the heat pipe does not exceed 150 W.

whereupon the signal goes to measuring input of digital oscilloscope 13. The oscilloscope is connected to the computer 14 via USB-interface.

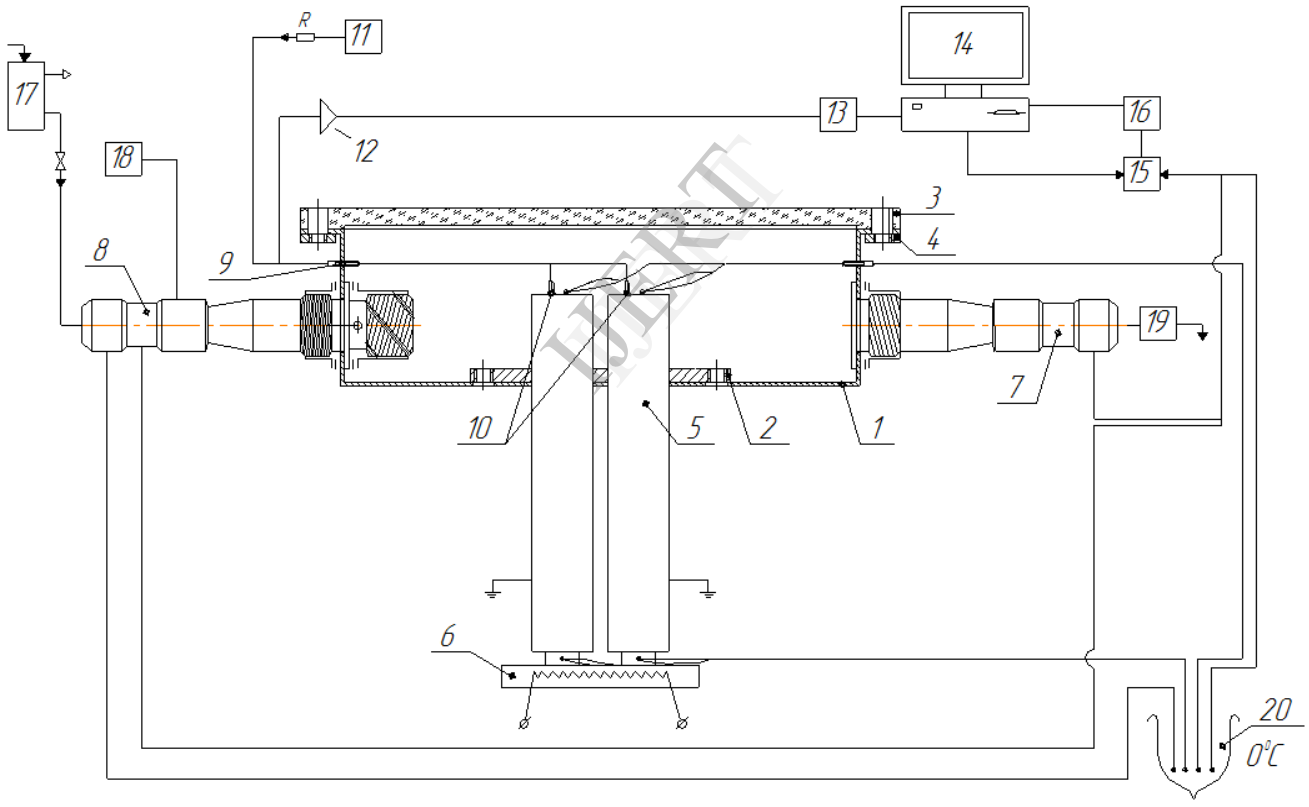

Fig.2. 1 — vortical continuous-flow calorimeter; 2 — heat pipes bolting flange; 3 — glass cover; 4 — cover fastening; 5 — heat pipes; 6 — resistance heater; 7 — outlet stub tube for water flow; 8 — inlet stub tube for water flow; 9 — silicone sealant of the sensing wire; 10 — capacitive sensors for measuring the thickness of the condensed layer of the working fluid; 11 — digital generator; 12 — power assist element; 13 — digital oscilloscope; 14 — computer; 15 — commutation switch; 16 — digital voltmeter; 17 — container for constant water head; 18 — source of air bubble; 19 — water flow meter; 20 — vacuum-jacketed container.

Fig. 3 shows measured data of modulation frequency response characteristics of heat pipes at various overheat δT values of evaporators.

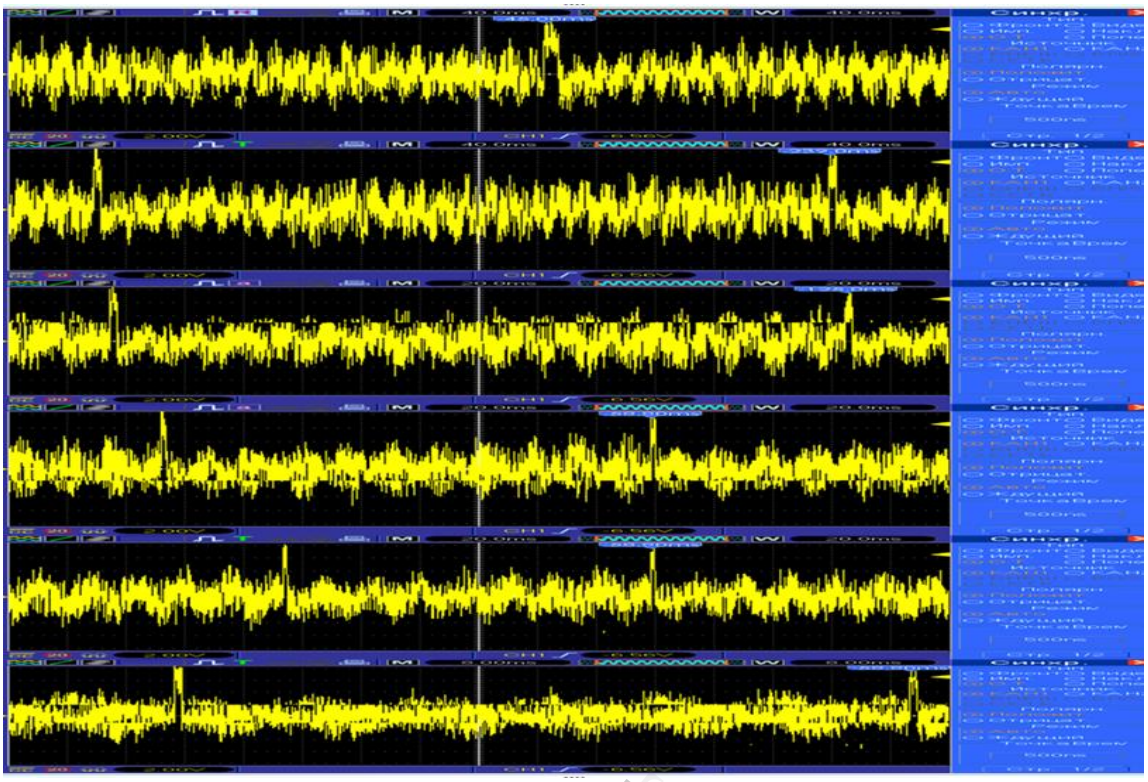

Fig.3. Waveforms of increase of modulation frequency depending on thermal load on heat pipe.

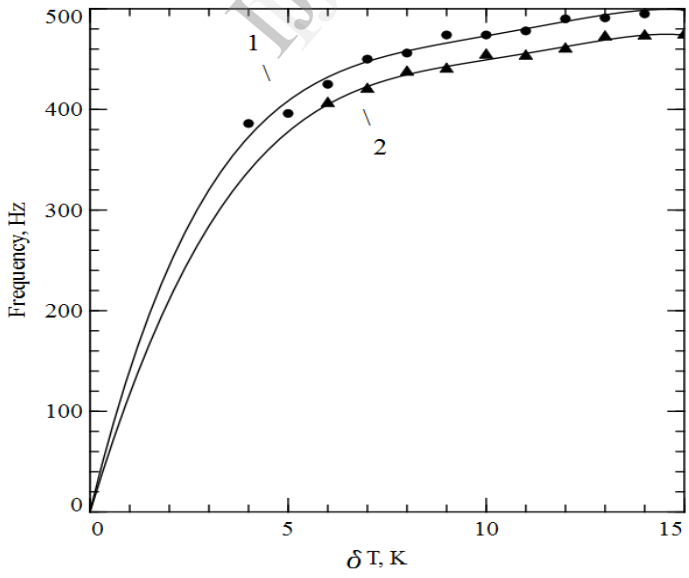

Fig.4. Test values of modulation frequency depending on overheating of heat pipe's evaporator, with reference to boiling temperature of diethyl ether 35.4°C.

1 — a heat pipe with the vapour channel close to the Laval nozzle;

2 — a heat pipe with a standard cylindrical vapour channel.

Both HPs have equal outer diameters and equal sectional areas of capillary-porous inserts near the condensation region.

Initial pulsed flows occur in HP with the nozzle, similar to the Laval nozzle, in event of overheating of the evaporator δT~4K, frequency (modulation frequency of electromagnetic pulsation) f ~386 Hz.

As the overheating of the evaporator δT~ 15K increases, pulsation frequency in the nozzle goes event of overheating of the evaporator δT~6K, frequency (modulation frequency of electromagnetic pulsation) f ~406 Hz. As the overheating of the evaporator δT~15K increases, pulsation frequency in the cylindrical vapour channel goes up to 474 Hz, derivative of the relationship between pulsation frequency and temperature is approximately 7.5 Hz/K.

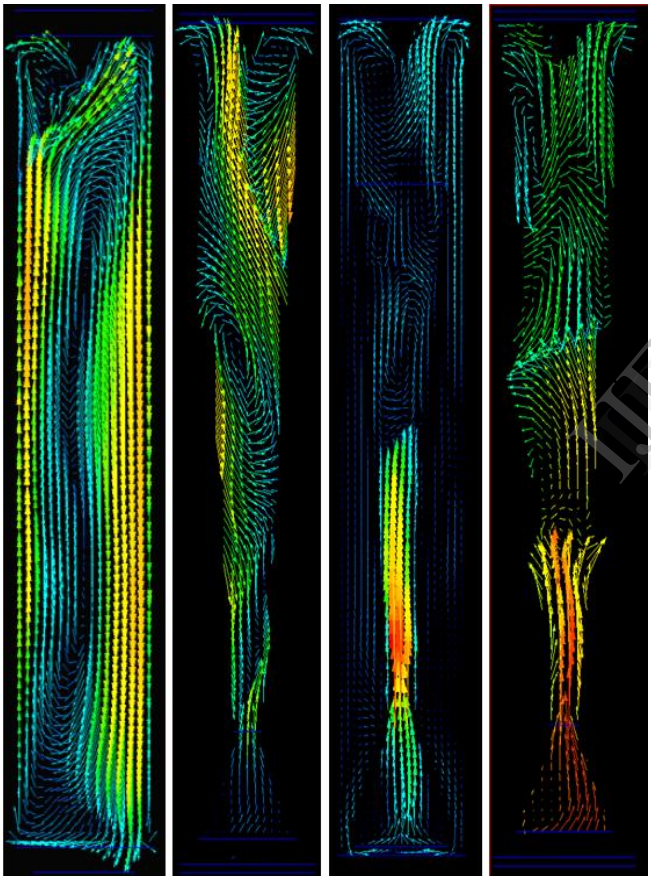

The insensitivity zone of the capacity sensors in the cylindrical channel, defined by the initial convective nature of the vapour flow, is greater than in the vapour channel, similar to the Laval nozzle.

Evaporation cycle in HPs exist at low heat load of the evaporator, up to 10-15 W/cm^2, and is characterized by convective flow in the vapour channel.

up to ~ 502 Hz, derivative of the relationship between pulsation frequency and temperature is approximately 10.5 Hz/K. While investigating HPs with standard cylindrical vapour channel and equal outer diameter 20 mm, length 100 mm and thickness of the evaporator and capillary-porous insert 3 mm, initial pulsed flows occur in

Dynamic range of pulsations in the HP's vapour channel, similar to the Laval nozzle, is a little greater in frequency, in comparison to dynamic range of pulsations 406 Hz – 474 Hz in cylindrical vapour channel, and equals to 386 Hz – 502 Hz. Measuring inaccuracy does not exceeds 3-5 Hz.

The results of flow simulation of compressible supersaturated vapour environment inside a vapour channel, in the form of a nozzle close to the Laval nozzle.

Fig.5. Test values of the vapour flow pulsation in the vapour channel of heat pipes as overheating of heat pipe's evaporator is increased in reference to boiling temperature of diethyl ether (35.4°C) by 1°C; 3°C; 5°C; and 7°C. The vapour flow velocity calculation was carried out using finite element modeling in CFD Design 10.0. Navier-Stokes and heat-transfer equations with measured boundary conditions were solved, i.e. using fixed temperature values of heat source and heat outlet.

The model was studied as a longitudinal section along the axes of the two injector channels, which helps to preserve all the specific features of whirling instability under the conditions of continuous circulation motion of the working fluid during liquid and vapor phases.

In the construction of the design model about 502301 finite elements were used, with increased meshing at injection capillary channels sections, nozzle throat section and turbulence element. The model size is a compromise between available computer resources and computational investigation error. Is clearly visible transition from stationary convective flow regime in the vapour channel to pulsatile flow regime.

Evaporation cycle of short HPs, when evaporator heating power is constant and maximum value is limited to prevent the development of bubble

boiling in the flat grid evaporator, is defined in the following way:

$$E = \frac{\Delta Q}{\Delta \tau} < E_B \quad (1)$$

Rate of evaporation of dry monomolecular vapour over the evaporator is defined by the following equation:

$$\dot{M} = \dot{n}_{vp} m_{vp} = \frac{E}{r(T_B)} \quad (2)$$

Mass flow of saturated dry monomolecular vapour over the evaporator is defined by the following equation:

$$G_{vp} = \dot{M} = F(z)\rho_{vp}(T_{ev})u_{vp} = \frac{E}{r(T_B)} \quad (3)$$

Growth rate of the number of molecules of vapour over the evaporator in the convergent region of the nozzle of the vapour channel, which defines excess pressure over the evaporator and mass flow of vapour in HP, is calculated from the equation:

$$\dot{n}_{vp} = \frac{E}{r(T_B)m_{vp}} = \frac{EN_A}{r(T_B)\mu_{vp}} \quad (4)$$

Assuming approximately equal velocities and without considering the jet type nature of the flow pattern, the linear velocity of the hydrodynamic flotation of the vapour flow over the evaporator surface is calculated from the equation:

$$u_{vp} \simeq \frac{\dot{n}_{vp}}{F(z)n_{vp}(T_{ev})} = \frac{EN_A}{F(z)r(T_B)\mu_{vp}n_{vp}(T_{ev})} \quad (5)$$

Insert expressions (5) and (4) in the equation (3) to obtain the formula for calculation of molecular flow of the dry vapour over the evaporator:

$$G_{vp} \simeq \rho_{VP}(T_{ev})\frac{EN_A}{r(T_B)\mu_{vp}n_{vp}(T_{ev})} \quad (6)$$

Hydrodynamic flow of saturated dry vapour is defined by pressure difference value between the evaporator and condensation region in HP, according to the formula:

$$G_{vp} \simeq A\frac{\rho_{vp}(T_{cond})F(z)^2[P(T_{ev})-P(T_{cond})]}{\eta L} \quad (7)$$

Equate mass and hydrodynamic flow of saturated dry vapour, and obtain the following equation:

$$A\frac{\rho_{vp}(T_{cond})F(z)^2\Delta P_{vp}}{\eta L} \simeq \rho_{VP}(T_{ev})\frac{EN_A}{r(T_B)\mu_{vp}n_{vp}(T_{ev})} \quad (8)$$

Excess pressure over the evaporator defines transfer of the vapour flow in the vapour channel of the HP, and is calculated in linear approximation according to the equation:

$$P(T_{ev}) \simeq P(T_{cond}) + \frac{dP}{dT}(T_{ev} - T_{cond}) \quad (9)$$

With respect to the Clapeyron-Clausius equation, pressure derivative of the vapour by temperature is calculated in a conventional manner, nevertheless considering the fact that for liquid the specific volume ratio is small, $v^L / v^{VP} < 10^{-2} - 10^{-3}$, hence in the Clapeyron-Clausius equation the value of the specific volume of fluid v^L is ignored, and in ideal gas state the following equation is obtained:

$$\frac{dP}{dT} = \frac{1}{T}\frac{r(T_B)}{(v^{VP} - v^L)} \simeq \frac{r(T_B)}{T_{cond}}\rho_{vp}(T_{cond}) \quad (10)$$

Substitute expression (10) in (8), and obtain the equation to calculate vapour quantity in the HP:

$$\frac{F(z)^2}{\eta L}\frac{r(T_B)}{T_{cond}}\rho_{vp}(T_{ev} - T_{cond}) \simeq \frac{EN_A}{r(T_B)\mu_{vp}n_{vp}(T_{ev})} \quad (11$$

Vapour temperature over the evaporator's surface with low evaporation and without boiling is defined by the equation (12):

$$T_{ev} \simeq T_{cond}\left(1 + \frac{EN_A\eta L}{\rho_{vp}(T_{cond})F(z)^2r(T_B)^2\mu_{vp}n_{vp}(T_{ev})}\right) \leq T_B \quad (12)$$

Steady-state evaporation conditions in HP mean that the temperature in the evaporator does not exceed boiling temperature of the working fluid. Heating capacity of the HP, W, is defined according to the following equation:

$$\frac{\rho_{vp}(T_{cond})F(z)^2r(T_B)^2\mu_{vp}n_{vp}(T_{cond})}{N_A\eta L T_{cond}}(T_{ev} - T_{cond}) \simeq \simeq K_{HP}\Delta T \quad (13)$$

Heat transfer coefficient at cross-section of the vapour channel of the HP is defined according to the following expression:

$$K_{HP} \simeq \frac{\rho_{vp}(T_{cond})F(z)^2 r(T_B)^2 \mu_{vp} n_{vp}(T_{cond})}{N_A \eta L T_{cond}} \quad (14)$$

When the rate of heat supply into the thin evaporator is high, its average temperature is greater than the boiling temperature of the working fluid during bubble boiling or vapourization. The hydrodynamic vapour flow at the converging region of the nozzle has no time to carry out heating capacity generated through boiling in the evaporator. Vapour density and pressure increase and boiling temperature of the working fluid goes up until it exceeds average temperature of the evaporator. Upon pressure increase the boiling in the evaporator stops (slows), and an overpressure wave spreads in the vapour channel to the condensation region of the HP, where the vapour becomes supersaturated, and condenses. The condensation process is not instant, and when the evaporator's activity is slowed (stopped), condensation lasts until the pressure decreases to the vapour saturation pressure at the condensation temperature, thereafter the condensation process stops. The slow process of saturated vapour pressure decrease, due to condensation, feeds back through the vapour channel of the HP back to the evaporator, and the boiling process there is resumed. Pressure pulsations in the vapour channel of the HP result from boiling and intensive vapour generation in the evaporator, non-instantaneous mass-transfer through the vapour channel to the condensation region of the HP, and the slow condensation process, which provides pressure decrease in the condensation region at first and then in the evaporator of the HP. Following all described processes the next pulsed evaporation cycle is resumed.

The heating capacity, entering to the flat grid evaporator of the short HP, when the evaporator's temperature exceeds the boiling temperature $T_B(p)$ of the working fluid, is defined according to the next equation:

$$E = \frac{[T_{ev} - T_B(p)]F(z)}{R_{ev}(T)} \quad (15)$$

It is considered that moist vapour is formed of two subsystems: microdrops system and dry vapour system. Rate of vaporization of the moist droplet vapour flow is defined in the standard way:

$$\dot{M} = G_{mix} = G_{vp} + G_{dr} \quad (16)$$

For the purpose of simplification of the analytical model construction, the real droplet vapour flow over the evaporator - having microdrops dimensioned by complicated double-humped distribution function [6] - is reported in terms of a mono-dispersal system of spherical microdrops with arithmetic middling radius r_a, which is frequently used while analyzing two-phase droplet vapour flows:

$$r_a = \frac{1}{n_{dr}} \sum_{i=0}^{\infty} r_{dri} n_{dri} \quad (17)$$

Considering the accepted assumption over spherical shape of microdrops, the expression for absolute moisture of the droplet vapour flow:

$$\gamma = \frac{M_{dr}}{M_{dr} + M_{vp}} = \left[1 + \frac{\rho_{vp}}{\rho_L}\left(\frac{3}{4\pi} \frac{1}{r_a^3 n_{dr}} - 1\right)\right]^{-1} \quad (18)$$

Synergies between consumable and absolute mass concentrations of microdrops or consumable and absolute moisture are defined according to the following relation:

$$\gamma_G = \frac{\gamma\psi}{(1-\gamma)+\gamma\psi}; \quad \psi = \frac{u_{dr}}{u_{vp}} \quad (19)$$

The value γ_G represents the relation between quantity of the condensed droplet phase and total quantity of the two-phase droplet vapour, and, considering the expression (23) is as follows:

$$\gamma_G = \left[1 + \frac{\rho_{vp}}{\rho_L \psi}\left(\frac{3}{4\pi} \frac{1}{r_a^3 n_{dr}} - 1\right)\right]^{-1} = \frac{G_{dr}}{G_{mix}} \quad (20)$$

Mass flow rate of microdrops on the evaporator's surface are considered to be proportional to vaporization velocity and mass flow rate of the vapour:

$$G_{dr} \approx B\left(\frac{E}{r(T_B)}\right)^a \left(\frac{G_{vp}}{F}\right)^b \quad (21)$$

To evaluate the vapour quantity transported from the evaporator to the condensation region of the HP, equation (7) is used, where the microdrops subsystem contribution to the generation of overpressure of the two-phase droplet mixture over the evaporator $P(T_{ev})$ in the vapour channel of the is neglected:

$$G_{mix} = G_{vp} + G_{dr} \simeq$$

$$A\frac{\rho_{vp}^{mix}(T_{ev})F(z)[P(T_{ev}) - P(T_{cond})]}{\eta_{mix} L} = \frac{\rho_{vp}^{mix} F(z)\Delta P_{vp}}{\eta_{mix} L} \quad (22)$$

As a result of the boiling process in the evaporator, the pressure of the vapour over the evaporator increases up to P^*, whereby the boiling process in the surface layers and further in the whole of the thin evaporator (3mm thick) is slowed (stopped) due to the fact that average temperature of the evaporator T_{ev} becomes lower than the boiling temperature of the working fluid in the evaporator under the increased pressure and the confined spaces

$$T_{ev} < T_B(P^*) \quad (23)$$

Furthermore, pulsing of the overpressured vapour begins to spread to the condensation region through the vapour channel.

Cessation of boiling and retarding of vaporization in the evaporator of the HP lead to significant reduction (cessation) of the heat release and decrease in moist vapour transportation along the vapour channel of the HP to the condensation region of the HP.

The time period $\Delta\tau_{ev}$ of pressure increase up to P^* and cessation of boiling in the capillary-porous evaporator is estimated in linear approximation in ideal gas state and laminar heat transfer inside of the vapour channel of the HP, according to the formula:

$$\Delta\tau_{ev} \simeq \frac{[P^* - P(T_{cond})]F(z)L}{k_B T_{ev} \dot{n}_{vp}} \simeq \frac{[P^* - P(T_{cond})]F(z)Lr(T_B)m_{vp}}{Ek_B T_{ev}} \quad (24)$$

Surplus energy (increased pressure) release time in the evaporating region, by means of vapour flow transfer to the condensation region of the HP, is estimated according to the following formula:

$$\Delta\tau_{HP} \simeq \frac{E\Delta\tau_{ev}}{r(T_B)\rho_{vp}^{mix}(T_{ev})u(T_{ev})F(z)} \quad (25)$$

Surplus pressure release time $\Delta\tau_{HP}$ partially determines the time value of oscillations of the vapour flow in the vapour channel of the HP, during which the vapour pressure pulse, initiated over the evaporator, reaches the HP condensation surface, and condenses partially. The time period $\Delta\tau_{cond}$ of pressure decrease up to $P(T_{cond})$ is estimated according to the formula:

$$\Delta\tau_{cond} \simeq \frac{E\Delta\tau_{ev}}{r(T_{cond})\rho_{vp}^{mix}(T_{cond})u(T_{cond})F(z)} \quad (26)$$

As a result of the liquid phase formation, pressure near the cooling condensation surface reduces to:

$$P^* \simeq P(T_{cond}) \quad (27)$$

This leads to the slowing of heat transfer through the vapour channel, the rarefaction wave propagation from the condensation zone to the evaporator and the start of the next cycle of pulsed increase of the pressure near the evaporator's surface.

Thus, cycle pulse duration $\Delta\tau_0$ in the vapour channel of the HP:

$$\Delta\tau_0 \simeq \Delta\tau_{ev} + \Delta\tau_{HP} + \Delta\tau_{cond} + \Delta\tau_{sound} \quad (28)$$

Pulse frequency:

$$\nu \simeq \frac{1}{\Delta\tau_{ev} + \Delta\tau_{HP} + \Delta\tau_{cond} + \Delta\tau_{sound}} \quad (29)$$

The analysis of the obtained measured data of heat transfer over the evaporator shows that working of the designed heat pipes is based on the boiling regime. This fact is confirmed by influences of operating parameters of the vapourisation process (q, p) on the heat transfer coefficient α. The influence of these parameters is related to the similar influence of the heat flow density and pressure over the bubble boiling in the substantial volume.

Pulsed regime occurs in heat pipes when boiling of the working fluid in the evaporator.

Measured data provides the value of time period of pulsations in the vapour channel of the HP about ~ 10^{-3}s.

CONCLUSIONS

The pulsatile flow regime in the vapour channel occurs when the working fluid in the evaporator starts to boil. Vapour density and pressure increase and boiling temperature of the working fluid goes up until it exceeds average temperature of the evaporator. Upon pressure increase the boiling in the evaporator stops (slows), and an overpressure wave spreads in the vapour channel to the condensation region of the HP, where the vapour becomes supersaturated, and condenses.

Flow stagnation leads to vortex formation, and their interaction causes pulse-coupled vortex decay, static pressure boost and complex reverse flows. Calculation results show that flow stagnation during the pulsation cycle leads to an enlargement of the recirculating region and augmentation of condensation, and this effect is significant. With all the operating parameters of heat pipes, two effects were observed: pulsating flow regime of two-phase vapour flow and film-type condensation.

Heat transfer coefficient of the short heat pipe with the vapour channel, in the form close to the Laval nozzle, is $(18\pm1)\cdot10^4$ W/m^{2}K; heat transfer coefficient of the pipe with the cylindrical vapour channel is $(15\pm1)\cdot10^4$ W/m^{2}K, if thickness of the capillary-porous insert layer is 3 mm [4-5].

Heat resistance of heat pipes with a vapour channel in the form of a nozzle is 0.028±0.01 K/W, heat resistance of heat pipes with a standard cylindrical vapour channel is 0.032±0.01 K/W.

NOMENCLATURE

E — heat capacity, supplied in the evaporator of the HP, W;
ΔQ — heat energy, absorbed in the evaporator over a period of $\Delta\tau$, J;
$\Delta\tau$ — unit time, s;
E_B — heat capacity, wherein the process of bubble boiling begins in the grid evaporator W;
$\dot{M}$ — the amount of the dry vapour, generated over the evaporator per unit time, kg/s;
$\dot{n}_{vp}$ — growth velocity of the number of vapour molecules over the evaporator per unit time, s^{-1};
m_{vp} — mass of molecule of diethyl ether, kg;
$r(T_B)$ — specific vapourization heat of the working fluid in the heat pipe, in the general case, depend upon temperature and pressure, J/kg;
$r(T_{cond})$ — specific vapourization heat of the working fluid in the heat pipe near the condensation surface, J/kg;
G_{VP} — mass flow of dry saturated vapour over the evaporator, kg/s;
G_{mix} — mass flow of moist saturated vapour over the evaporator, kg/s;
G_{dr} — mass flow of microdrops of the saturated vapour over the evaporator, kg/s;
F(z) — surface area of the evaporator inside the vapour channel of the heat pipe, m^2;
z — longitudinal coordinate along the centroidal axis of the heat pipe, m;
$n_{vp}(T_{ev})$ — average number of dry vapour molecules in the unit volume of the vapour channel over the evaporator, m^{-3};
u_{vp} — average velocity of hydrodynamic flotation of the dry vapour over the evaporator, m/s ;
$\rho_{VP}(T_{ev})$ — vapour density of diethyl ether over the evaporator, kg/m^3;
$\rho_{VP}(T_{cond})$ — vapour density of diethyl ether near the condensation surface, kg/m^3;
$\rho_{vp}^{mix}(T_{ev})$ — moist vapour density of diethyl ether over the evaporator, kg/m^3;
$\rho_{vp}^{mix}(T_{cond})$ - moist vapour density of diethyl ether near the condensation surface, kg/m^3;
ν^{VP} — specific volume of the saturated vapour, m^3/kg;
ν^{L} — specific volume of the working fluid on the liquid-vapour coexistence line, m^3/kg,
N_A — Avogadro constant, mol^{-1};
μ_{vp} — molar mass of diethyl ether vapour, kg/mol;
A — nondimensional constant about a unit ;

$P(T_{ev})$ — vapour pressure near the surface of the evaporator of the heat pipe, Pa;
$P(T_{cond})$ — vapour pressure near the condensation surface of the heat pipe, Pa;
P^* — vapour pressure over the surface of the evaporator, which stops the process of boiling in the capillary-porous evaporator, Pa;
k_B – Boltzmann's constant, $k_B = 1.38065 \cdot 10^{-23}$ J/K;
η — coefficient of dynamic viscosity of the dry vapour, Pa·s;
η_{mix} — coefficient of dynamic viscosity of the moist vapour with microdrops, Pa·s;
L — the length of the vapour channel of the heat pipe, m;
ΔP_{vp} — vapour pressure difference over the evaporator and near the condensation surface in the vapour channel of the heat pipe, Pa;
T_{ev} — temperature of the surface of the evaporator, K;
T_{cond} — temperature of the condensation surface , K;
$T_B(P)$ — boiling temperature of the working fluid, K;
dP/dT — pressure derivative with respect to temperature of diethyl ether of the working fluid within the heat pipe, Pa/K;
K_{HP} — heat transfer coefficient through the cross section of the vapour channel of the heat pipe, W/K;
$R_{ev}(T)$ — heat resistance of the flat evaporator, including outer wall of the heat pipe, $K/W/m^2$;
r_a — arithmetic middling radius of microdrops in two-phase droplet vapour flow, m;
r_{dri} — radius of the i microdrop in the unit volume of the droplet vapour flow over the evaporator, m;
n_{dri} — number of microdrops of the working fluid with radius r_{dri} per unit volume of the droplet vapour medium, $1/m^3$;
n_{dr} — total number of microdrops of all sizes per unit volume of the droplet vapour flow over the evaporator, $1/m^3$;
γ — absolute moisture degree of the droplet vapour flow;
M_{dr} — total mass of microdrops per unit volume of the droplet vapour flow over the evaporator, kg;
M_{vp} — vapour mass per unit volume of the droplet vapour flow over the evaporator, kg;
ρ_{vp} — density of the dry vapour, kg/m^3;
ρ_L — density of microdrops of the working fluid, kg/m^3;
γ_G — degree of moisture discharge of the droplet vapour flow;
ψ — phase slip ratio of the droplet vapour flow, equal to the relation between average velocities of the microdrops movement and the vapour phase ;
u_{dr} — average velocity of the microdrops movement in the vapour flow, m/s;
u_{vp} — average velocity of the vapour phase, m/s;
B — coefficient with account for thermophysical properties of the working fluid and structural parameters of the evaporator (porosity, typical dimension of channels and pores);
a ans b — numerical coefficients;
P^* — increased vapour pressure of the working fluid, wherein the boiling process in the surface layers of the evaporator stops, Pa;
$\Delta\tau_{ev}$ — cycle duration of pressure increasing prior to the cessation of the boiling process in the evaporator, s;
$\Delta\tau_{HP}$ — duration of pressure pulse propagation through the vapour channel of the heat pipe, s;
$\Delta\tau_{cond}$ - cycle duration of pressure decrease due to condensation near the condensation surface of the heat pipe, s;
$\Delta\tau_0$ — cycle pulse duration, s.

REFERENCES

1. Gupta A.K., Lill1ey D.G., Syred N. Swirl Flows. Abacus Press. 1984. 588p.
2. Patent for useful model N.95812 RF, F28D 15/00/Device for heat pipe filling with non-wettable fluid. Seryakov A.V. Published 10. 07. 2010. Bulletin 19.
3. Patent N 2431101 RF, F 28D 15/00/ Method of heat pipe filling. Seryakov A.V. Published 10. 10. 2011. Bulletin 28.
4. Seryakov A.V., Konkin A.V., Belousov V.C. The use of the jet vapour nozzle in medium-temperature range heat pipes.// Siberian State Aerospace University Bulletin. 2012. Number 1(41), p.142-147.
5. Seryakov A.V. Velocity measurements in the vapour channel of low temperature range heat pipes// International Journal of Engineering Research & Technology 2013, v.2, № 8, pp. 1595 – 1603.
6. Lee R., Reges J., Almenas K. Size and number density change of droplet populations above front during reflood // International Journal of Heat and Mass Transfer. 1984. v.27. N4. p. 573-585.